



1 **Highly branched isoprenoids for Southern Ocean semi-**
2 **quantitative sea ice reconstructions: a pilot study from the**
3 **Western Antarctic Peninsula**

4
5 Maria-Elena Vorrath¹, Juliane Müller^{1,2,3}, Oliver Esper¹, Gesine Mollenhauer^{1,2}, Christian
6 Haas¹, Enno Schefuß², Kirsten Fahl¹

7 ¹Alfred Wegener Institute, Helmholtz Centre for Polar and Marine Research, Bremerhaven, Germany

8 ²MARUM – Center for Marine Environmental Sciences, University of Bremen, Germany

9 ³Department of Geosciences, University of Bremen, Germany

10 *Correspondence to:* Maria-Elena Vorrath, maria-elena.vorrath@awi.de

11
12 **Abstract.** Organic geochemical and micropaleontological analyses of surface sediments collected in the southern
13 Drake Passage and the Bransfield Strait, Antarctic Peninsula, enable a proxy-based reconstruction of recent sea
14 ice conditions in this climate sensitive area. The distribution of the sea ice biomarker IPSO₂₅ supports earlier
15 suggestions that the source diatoms seem to be common in near-coastal environments characterized by an annually
16 recurring sea ice cover. We here propose and evaluate the combination of IPSO₂₅ with a more unsaturated highly
17 branched isoprenoid alkene and phytosterols and introduce the PIPSO₂₅ index as a potentially semi-quantitative
18 sea ice proxy. This organic geochemical approach is complemented with diatom data. PIPSO₂₅ sea ice estimates
19 are used to discriminate between areas characterized by permanently ice-free conditions, seasonal sea ice cover
20 and extended sea ice cover. These trends are consistent with satellite sea ice data and winter sea ice concentrations
21 estimated by diatom transfer functions. Minor offsets between proxy-based and satellite-based sea ice data are
22 attributed to the different time intervals recorded within the sediments and the instrumental records from the study
23 area, which experienced rapid environmental changes during the past 100 years.

24
25 Key Words: biomarker, IPSO₂₅, sea ice, Bransfield Strait, satellite observation

26 **1 Introduction**

27 In the last century, the Western Antarctic Peninsula (WAP) has undergone a rapid warming of the atmosphere of
28 $3.7 \pm 1^\circ \text{C}$, which exceeds several times the average global warming (Vaughan et al., 2003). Simultaneously, a



1 reduction in sea ice coverage (Parkinson and Cavalieri, 2012), a shortening of the sea ice season (Parkinson, 2002)
2 and a decreasing sea ice extent of ~4–10 % per decade (Liu et al., 2004) are recorded in the adjacent Bellingshausen
3 Sea. The loss of seasonal sea ice and increased melt water fluxes impact the formation of deep and intermediate
4 waters, the ocean-atmosphere-exchange of gases and heat, the primary production and higher trophic levels
5 (Arrigo et al., 1997; Orsi et al., 2002; Anderson et al., 2009). Since the start of satellite-based sea ice observations,
6 however, a slight increase in Antarctic sea ice extent has been documented, which contrasts the significant decrease
7 of sea ice in Western Antarctica, especially around the WAP (Hobbs et al., 2016).

8 For an improved understanding of the oceanic and atmospheric feedback mechanisms associated with the observed
9 changes in sea ice coverage, reconstructions of past sea ice conditions in climate sensitive areas such as the WAP
10 are of increasing importance. A common approach for sea ice reconstructions in the Southern Ocean is based on
11 the investigation of sea ice associated diatom assemblages preserved in marine sediments (Bárcena et al., 1998;
12 Gersonde and Zielinski, 2000; Heroy et al., 2008; Leventer, 1998; Minzoni et al., 2015). By means of transfer
13 functions, this approach can provide quantitative estimates of a paleo sea ice coverage (Crosta et al., 1998; Esper
14 and Gersonde, 2014a). The application of diatoms for paleoenvironmental studies, however, can be limited by the
15 selective dissolution of biogenic opal frustules (Burckle and Cooke, 1983; Esper and Gersonde, 2014b), especially
16 in surface sediments (Leventer, 1998). As an alternative or additional approach to diatom studies, Massé et al.
17 (2011) proposed the use of a specific biomarker lipid – a diunsaturated highly branched isoprenoid alkene (HBI
18 C_{25:2}, Fig. 1) – for Southern Ocean sea ice reconstructions. The HBI diene was first described by Nichols et al.
19 (1988) from sea ice diatoms. ¹³C isotopic analyses of this HBI diene suggest a sea ice origin for this molecule
20 (Sinninghe Damsté et al., 2007; Massé et al., 2011) and this is further corroborated by the identification of the sea
21 ice diatom *Berkeleya adeliensis* as a producer of this HBI diene (Belt et al., 2016). In a survey of surface sediments
22 collected from proximal sites around Antarctica, Belt et al. (2016) note a widespread sedimentary occurrence of
23 the HBI diene and – by analogy with the Arctic HBI monoene termed IP₂₅ (Belt et al., 2007) – proposed the term
24 IPSO₂₅ (Ice Proxy for the Southern Ocean with 25 carbon atoms) as a new name for this biomarker.

25 In previous studies, a HBI triene (HBI C_{25:3}; Fig. 1) found in polar and sub-polar phytoplankton samples (Massé
26 et al., 2011) has been considered alongside IPSO₂₅ and the ratio of IPSO₂₅ to this HBI triene hence has been
27 interpreted as a measure for the relative contribution of organic matter derived from sea ice algae versus open
28 water phytoplankton (Massé et al., 2011; Collins et al., 2013; Etourneau et al., 2013; Barbara et al., 2013, 2016).
29 Collins et al. (2013) further suggested that the HBI triene might reflect phytoplankton productivity in marginal ice
30 zones (MIZ) and, based on the observation of elevated HBI triene concentrations in East Antarctic MIZ surface
31 waters, this has been strengthened by Smik et al. (Smik et al., 2016a). Known source organisms of C_{25:3} HBI trienes



1 (Fig. 1 shows molecular structures of both E- and Z-isomer) are, for example, *Rhizosolenia* and *Pleurosigma*
2 diatom species (Belt et al., 2000, 2017). In the Arctic Ocean, the HBI Z-triene has been used to further modify the
3 so-called PIP₂₅ index (Smik et al., 2016b) - an approach for semi-quantitative sea ice estimates. Initially, PIP₂₅ was
4 based on the employment of plankton-derived phytosterols, such as brassicasterol and dinosterol (Kanazawa et al.,
5 1971; Volkman, 2003), to serve as open-water counterparts, while IP₂₅ reflects the occurrence of a former sea ice
6 cover (Belt et al., 2007; Müller et al., 2009, 2011). Consideration of these different types of biomarkers helps to
7 discriminate between ice-free and permanently ice-covered ocean conditions, both resulting in a lack of IP₂₅ and
8 IPSO₂₅, respectively (for further details see Belt, 2018; Belt and Müller, 2013a). Uncertainties in the source-
9 specificity of brassicasterol (Belt et al., 2013), however, require caution when pairing this sterol with a sea ice
10 biomarker lipid for sea ice reconstructions. While the applicability of HBIs (and sterols) to reconstruct past sea ice
11 conditions has been thoroughly investigated in the Arctic Ocean (Belt, 2018; Xiao et al., 2015), only two studies
12 document the distribution of HBIs in Southern Ocean surface sediments (Belt et al., 2016; Massé et al., 2011). The
13 circum-Antarctic data set published by Belt et al. (2016), however, does not report HBI triene abundances.
14 Significantly more studies so far focused on the use of IPSO₂₅ and the HBI Z-triene for paleo sea ice
15 reconstructions and these records are always compared to micropaleontological diatom analyses (Barbara et al.,
16 2013; Collins et al., 2013; Denis et al., 2010).

17 Here, we provide a first overview of the distribution of IPSO₂₅, HBI trienes, brassicasterol and dinosterol in surface
18 sediments from the northern part of the WAP (southern Drake Passage and Bransfield Strait). These biomarker
19 data are completed by diatom analyses and remote sensing sea ice data. We further introduce and discuss the so-
20 called PIPSO₂₅ index (phytoplankton-IPSO₂₅ index), which, following the PIP₂₅ approach in the Arctic Ocean
21 (Müller et al., 2011), may serve as a semi-quantitative indicator of past Southern Ocean sea ice cover. These
22 biomarker-based sea ice estimates are compared to sea ice concentrations derived from diatom transfer functions
23 and satellite-derived data on the recent sea ice conditions in the study area.



1 **2 Oceanographic setting**

2 The study area includes the southern Drake Passage and the Bransfield Strait located between the South Shetland
3 Islands and the northern tip of the WAP (Fig. 2a and b). While the oceanographic setting in the Drake Passage is
4 dominated by the Antarctic Circumpolar Current (ACC), a complex current system prevails in the Bransfield Strait.
5 According to Sangrà et al. (2011) a branch of the ACC enters the Bransfield Strait in the west, carrying transitional
6 waters under the influence of the Bellingshausen Sea (Transitional Bellingshausen Sea Water, TBW). The TBW
7 is characterized by a well-stratified, warm and fresh water mass. In the eastern part, transitional water from the
8 Weddell Sea (Transitional Weddell Sea Water, TWW) enters the Bransfield Strait through the Antarctic Sound
9 and from the Antarctic Peninsula (AP). It is significantly colder and saltier due to extended sea ice formation in
10 the Weddell Sea Gyre. The two water masses are separated by the Peninsula Front (Sangrà et al., 2011).

11



1 3 Materials and Methods

2 3.1 Sediment Samples and radiocarbon dating

3 In total, 26 surface sediment samples obtained by multicorers and box corers during the RV *Polarstern* cruise
4 PS97 (Lamy, 2016) were analyzed (Fig. 2, Table 1). All samples were stored frozen and in glass vials. The
5 composition of the sediments ranges from foraminiferal mud in the Drake Passage to diatomaceous mud with
6 varying amounts of ice rafted debris in the Bransfield Strait (Lamy, 2016).

7 ^{14}C radiocarbon dating of two samples from the PS97 cruise and one from the *Polarstern* cruise ANT-VI/2
8 (Fütterer, 1988) was conducted using the mini carbon dating system (MICADAS) at Alfred Wegener Institute
9 following the method of Wacker et al. (2010). The ^{14}C ages were calibrated to calendar years before present (cal
10 BP) using the Calib 7.1 software (Stuiver et al., 2018) with an estimated reservoir age of 1178 years, derived from
11 the six closest reference points listed in the Marine Reservoir Correction Database (www.calib.org).

12

13 3.2 Organic geochemical analyses

14 For biomarker analyses, sediments were freeze-dried and homogenized using an agate mortar. Prior to extraction,
15 internal standards 7-hexylnonadecane (7-HND) and 5 α -androstan-3 β -ol were added to the sediments. For the
16 ultrasonic extraction (15 min), a mixture of CH_2Cl_2 :MeOH (v/v 2:1; 6ml) was added to the sediment. After
17 centrifugation (2500 rpm for 1 min), the organic solvent layer was decanted. The ultrasonic extraction step was
18 repeated twice. From the combined total organic extract, apolar hydrocarbons were separated via open column
19 chromatography (SiO_2) using hexane (5 ml). Sterols were eluted with ethylacetate:hexane (v/v 20:80; 8 ml). HBIs
20 were analyzed using an Agilent 7890B gas chromatography (30 m DB 1MS column, 0.25 mm diameter, 0.250 μm
21 film thickness, oven temperature 60° C for 3 min, rise to 325° C within 23 min, holding 325° C for 16 min) coupled
22 to an Agilent 5977B mass spectrometer (MSD, 70 eV constant ionization potential, ion source temperature 230°
23 C). Sterols were analyzed on the same instrument using a different oven temperature program (60° C for 2 min,
24 rise to 150° C within 6 min, rise to 325° C within 56 min 40 sec). The identification of IPSO₂₅ and the HBI trienes
25 is based on comparison of their retention times and comparison with published mass spectra (Belt et al., 2000).
26 For the quantification, peak areas of the molecular ions of the HBIs in relation to those of 7-HND were used. An
27 external calibration for HBI diene and trienes was applied using a sample with known HBI concentrations from
28 the Lancaster Sound, Canada, to account for the different response factors of the HBI molecular ions (m/z 346;
29 m/z 348) and the fragment ion of 7-HND (m/z 266). The identification of sterols was based on comparison of their
30 retention times and mass spectra with those of reference compounds run on the same instrument. Comparison of
31 peak areas of individual analytes and the internal standard was used for sterol quantification. Absolute



1 concentrations of HBIs and sterols were normalized to total organic carbon contents (for TOC data see Cárdenas
2 et al., 2018).

3 The herein presented phytoplankton-IPSO₂₅ index (PIPSO₂₅) is calculated using the same formula as for the PIP25
4 index following Müller et al. (2011):

$$5 \quad PIPSO_{25} = \frac{IPSO_{25}}{IPSO_{25} + (c \times \text{phytoplankton marker})} \quad (1)$$

6 The concentration balance factor *c* (*c* = mean IPSO₂₅ / mean phytoplankton biomarker) is applied to account for
7 the high offsets in the magnitude of IPSO₂₅ and sterol concentrations.

8 Stable carbon isotope composition of IPSO₂₅, requiring a minimum of 50 ng carbon, was successfully determined
9 on five samples using GC-irm-MS. The ThermoFisher Scientific Trace GC was equipped with a 30m Restek Rxi-
10 5 ms column (0.25 mm diameter, 0.25 µm film thickness) and coupled to a Finnigan MAT 252 isotope ratio mass
11 spectrometer via a modified GC/C interface. Combustion of compounds was done under continuous flow in
12 ceramic tubes filled with Ni wires at 1000° C under an oxygen trickle flow. The same GC program as for the HBI
13 identification was used. The calibration was done by comparison to a CO₂ reference gas. The values of δ¹³C are
14 expressed in per mill (‰) against Vienna PeeDee Belemnite (VPDB) and the mean standard deviation was <0.9
15 ‰. An external standard mixture was measured every six runs, achieving a long-term mean standard deviation of
16 0.2‰ and an average accuracy of <0.1 ‰.

17

18 3.3 Diatoms

19 Details of the standard technique of diatom sample preparation were developed in the micropaleontological
20 laboratory at the Alfred Wegener Institute (AWI) in Bremerhaven and described by Gersonde and Zielinski (2000).
21 The counting procedure follows Schrader and Gersonde (1978) with a light microscope Zeiss Axioplan 2 at x1000
22 magnification.

23 Since *Chaetoceros* resting spores were highly abundant but not significant for diatom-based environmental
24 analyses applied in this study they were not considered for sea ice calculations. To determine the transfer function
25 for the winter sea ice cover after Esper and Gersonde (2014a), most emphasis was given to the abundance and
26 preservation of the sea ice indicative diatom species *Fragilariopsis curta* and *Fragilariopsis cylindrus*. Hereby,
27 the general preservation state of the diatom assemblages was moderate to good in the Bransfield Strait and
28 decreased towards the Drake Passage where it is moderate to poor. Cold water related diatom species known to
29 dwell in the vicinity of sea ice, like *Thalassiosira weissflogii* and *Porosira pseudodenticulata* (Scott and Thomas,
30 2005), were also abundant (Table 4).



1 Diatoms species of *Fragilariopsis kerguelensis* but also *Azpeitia tabularis*, *Eucampia antarctica*, *Thalassiosira*
2 *lentiginosa* (and traces of *Thalassiosira oliverana*) were considered to reflect ice free habitats.

3

4 **3.4 Sea ice data**

5 The mean monthly satellite sea ice concentration was derived from the DMSP satellite SSM/I passive microwave
6 radiometers and downloaded from the National Snow and Ice Data Center (NSIDC; Cavalieri et al., 1996). An
7 interval from 1980 to 2015 was used to generate an average sea ice distribution for each season, spring (SON),
8 summer (DJF), autumn (MAM) and winter (JJA).

9



1 4 Results and Discussion

2 4.1 Distribution of IPSO₂₅, HBI trienes and sterols

3 The sea ice biomarker IPSO₂₅ was detected in 14 samples, with concentrations ranging between 0.37 and 17.81
4 $\mu\text{g g}^{-1}$ TOC (Table 1). The HBI Z-triene was present in all 26 samples (0.33-26.86 $\mu\text{g g}^{-1}$ TOC) and the HBI E-
5 triene was found in 24 samples (0.15-13.87 $\mu\text{g g}^{-1}$ TOC). Brassicasterol was present in all measured samples with
6 concentrations ranging from 3.39 to 5017.44 $\mu\text{g g}^{-1}$ TOC while dinosterol was detected in 22 samples (0.0002-
7 1983.75 $\mu\text{g g}^{-1}$ TOC).

8 The distribution of IPSO₂₅ in the study area shows a clear northwest-southeast gradient (Fig. 3a) with
9 concentrations increasing from the continental slope and around the South Shetland Islands towards the continental
10 shelf. Maximum IPSO₂₅ concentrations are observed in the Bransfield Strait. According to Belt et al. (2016),
11 deposition of IPSO₂₅ is highest in area covered by landfast sea ice and platelet ice during early spring and summer.
12 We note that core sites PS97/068 to PS97/073 in the central and eastern Bransfield Strait are located too distal to
13 be covered by fast ice and assume that peak IPSO₂₅ concentrations at these sites may refer to the frequent drift and
14 melt of sea ice exported from the Weddell Sea into the Bransfield Strait. IPSO₂₅ was not detected in sediments
15 from the permanently ice-free areas in the Drake Passage.

16 Highest concentrations of both HBI trienes are found in the eastern Drake Passage and along the continental slope,
17 while their concentrations in the Bransfield Strait are rather low (Fig. 3b and c) suggesting unfavorable
18 environmental conditions (ocean temperature, sea ice cover) for their source diatoms.

19 Brassicasterol and dinosterol are enriched in the eastern part of the Drake Passage and, in contrast to the
20 observation made for HBI trienes, also in the eastern and central Bransfield Strait (Fig. 3d and e). Sediments
21 collected along the Hero Fracture Zone in the western Drake Passage (Fig. 2) contain only minor amounts of
22 biomarkers except for elevated brassicasterol concentrations observed at stations PS97/048-1 and 049-2 (Fig. 3d).
23 This part of the Drake Passage is mainly barren of fine-grained sediments and dominated by sands (Lamy, 2016),
24 which may point to intensive winnowing by ocean currents impacting the deposition and burial of organic matter.
25 We consider that also degradation of HBIs and sterols may affect their distribution within surface sediments.
26 Rontani et al. (2014a) report a higher sensitivity of tri-unsaturated HBIs to oxidation but also note that oxidation
27 conditions in pelagic environments (i.e. their source organisms' habitat) are not as significant as those within sea
28 ice. A low reactivity towards oxidative degradation processes is observed for IPSO₂₅ (Rontani et al., 2014b, 2011),
29 which supports the good preservation of this lipid in marine sediments. While these degradation studies are
30 commonly conducted on laboratory diatom cultures and phytoplankton cell suspensions, investigations into



1 degradation processes affecting HBIs and sterols within sediments would address an important knowledge gap
2 regarding in-situ biochemical modifications of the biomarker signal.

3 The $\delta^{13}\text{C}$ values of IPSO₂₅ are between -10.3‰ and -14.7‰ which is the commonly observed range for IPSO₂₅ in
4 surface sediments and sea ice derived organic matter (Massé et al., 2011, Belt et al., 2016), and contrasts the low
5 $\delta^{13}\text{C}$ values of marine phytoplankton and their lipids in Antarctic sediments (-38‰ to -41‰ after Massé et al.,
6 2011).

7 Contrary to the finding of elevated Z-triene concentrations in surface waters along an ice-edge (Smik et al., 2016a)
8 and earlier suggestions that this biomarker may be used as a proxy for MIZ conditions (Belt et al., 2015; Collins
9 et al., 2013), we observe highest concentrations of the Z- and E-triene at the permanently ice-free northernmost
10 stations in the eastern Drake Passage. This is also apparent for brassicasterol and dinosterol suggesting an open
11 marine (pelagic) source for these sterols. Moderate concentrations of HBI trienes at the continental slope along
12 the WAP and in the Bransfield Strait likely refer to primary production at the sea ice margin during spring and
13 summer indicating seasonal ice free waters in high production coastal areas influenced by upwelling (Gonçalves-
14 Araujo et al., 2015). The similarity in the distribution of the Z- and the E-triene in our surface sediments – the
15 latter of which so far is not often considered for Southern Ocean paleoenvironmental studies – supports the
16 assumption of a common diatom source for these HBIs (Belt et al., 2000, 2017). Since brassicasterol and dinosterol
17 are highly abundant in both seasonally ice covered Bransfield Strait and the ice-free Drake Passage, their use as
18 an indicator of open-marine conditions is questionable. Elevated concentrations of both sterols in the Bransfield
19 Strait could either point to an additional input of these lipids from melting sea ice (Belt et al., 2013) or a better
20 adaptation of their source organisms to cooler and/or ice-dominated ocean conditions. Production and
21 accumulation of these lipids in (late) summer (i.e. after the sea ice season) may be considered as well. This
22 observation highlights the need for a better understanding of the source organisms and the mechanisms involved
23 in the synthesis of these sterols.

24

25 **4.2 A novel sea ice index for the Southern Ocean: PIPSO₂₅**

26 The main concept of combining the ice proxy with an indicator of an ice-free ocean environment (i.e. a
27 phytoplankton biomarker, Müller et al., 2011), aims at a semi-quantitative assessment of the sea ice conditions.
28 By reducing the light penetration through the ice, a thick and perennial sea ice cover limits the productivity of
29 bottom sea ice algae (Hancke et al., 2018), which results in the absence of both, sea ice and pelagic phytoplankton
30 biomarker lipids in the underlying sediments. Vice versa, sediments from permanently ice-free ocean areas only
31 lack the sea ice biomarker but contain variable concentrations of phytoplankton biomarkers (Müller et al., 2011).



1 The co-occurrence of both biomarkers in a sediment sample suggests seasonal sea ice coverage promoting algal
2 production indicative of sea ice as well as open ocean environments (Müller et al., 2011).

3 Following the PIP₂₅-approach applied in the Arctic Ocean (Müller et al., 2011; Belt and Müller, 2013; Xiao et al.,
4 2015) we used IPSO₂₅, HBI triene and sterol data to calculate the PIPSO₂₅ index. Depending on the biomarker
5 reflecting pelagic (open ocean) conditions, we define P_ZIPSO₂₅ (using the Z-triene), P_EIPSO₂₅ (using the E-triene),
6 P_BIPSO₂₅ (using brassicasterol), and P_DIPSO₂₅ (using dinosterol). Since the concentrations of IPSO₂₅ and both HBI
7 trienes are in the same range, the application of the c-factor is not needed here. For the calculation of P_BIPSO₂₅
8 the c-factor is 0.0048, for P_DIPSO₂₅ it is 0.0137.

9 The PIPSO₂₅ values determined for the study area are 0 in the Drake Passage and increase to intermediate values
10 at the South Shetland Islands and the continental slope and reach highest values in the Bransfield Strait (Fig. 4a-
11 d). Minimum PIPSO₂₅ values are supposed to refer to a predominantly ice-free oceanic environment in the Drake
12 Passage, while moderate PIPSO₂₅ values mark the transition towards a marginal sea ice coverage at the continental
13 slope and around the South Shetland Islands. Elevated PIPSO₂₅ values in samples from the northern Bransfield
14 Strait refer to a higher – potentially lasting until summer – seasonal sea ice cover and ice-edge phytoplankton
15 blooms. This pattern reflects the oceanographic conditions of a permanently ice-free ocean north of the South
16 Shetland Islands and a seasonal sea ice zone at the WAP as described by Cárdenas et al. (2018). Both HBI triene-
17 based PIPSO₂₅ indices show constantly high values at the coast of the WAP of >0.7 (P_ZIPSO₂₅) and >0.8
18 (P_EIPSO₂₅), respectively, in the southern Bransfield Strait paralleling the southwest-northeast oriented Peninsula
19 Front described by Sangrà et al. (2011). This front is reported to act as a barrier for phytoplankton communities
20 (Gonçalves-Araujo et al., 2015) and is associated with the encounter between TWW carrying Weddell Sea sea ice
21 through the Antarctic Sound and the TBW. PIPSO₂₅ values based on the E-triene are about 0.2 higher compared
22 to P_ZIPSO₂₅, because of the generally lower concentrations of the E-triene (Table 1). The sterol-based PIPSO₂₅
23 values display a generally similar pattern as P_ZIPSO₂₅ and P_EIPSO₂₅, respectively, and we note a high comparability
24 between the P_EIPSO₂₅ and P_BIPSO₂₅ values ($r^2 = 0.73$). Some differences, however, are observed in the
25 southwestern part of the Bransfield Strait (station PS97/056) where P_BIPSO₂₅ indicates a lower sea ice cover and
26 in the central Bransfield Strait (stations PS97/068 and PS97/069) where P_BIPSO₂₅ and P_DIPSO₂₅ reflect only MIZ
27 conditions. The HBI-triene based PIPSO₂₅ indices hence seem to reflect the oceanographic conditions within the
28 Bransfield Strait more satisfactorily.

29



1 4.3 Comparison of satellite-derived modern sea ice conditions and biomarker data

2 Satellite-derived sea ice data were averaged over the time period from 1980 to 2015 for all four seasons (Table 2)
3 and are considered to reflect the modern mean state of sea ice coverage around the WAP. Results show that the
4 winter sea ice does not extend north of 61° S and winter sea ice concentrations vary between 1 % and 50 % in the
5 study area (contour lines in Fig. 4), while sea ice is nearly absent (< 5 %) in summer (Table 2).

6 Sea ice concentrations of up to 50 % are common in winter between the South Shetland Islands and north of the
7 Antarctic Sound where the influence of TWW is highest. Permanent sea ice cover is uncommon in the Bransfield
8 Strait and around the WAP and this area is mainly characterized by a high seasonality and low concentrations of
9 drift ice. Comparisons of individual biomarker concentrations with satellite sea ice data reveals a weak and positive
10 correlation between IPSO₂₅ concentrations and winter sea ice concentrations ($r^2 = 0.5$), while no correlation is
11 found between sea ice and pelagic biomarker concentrations ($r^2 < 0.1$ for all relations).

12 Correlations of PIPSO₂₅ values with satellite-derived sea ice concentrations (for spring, summer, autumn and
13 winter) contrast earlier observations made for the PIP₂₅ index in the Arctic Ocean, where the closest relationship
14 is found mainly with the spring sea ice coverage (i.e. the blooming season of sea ice algae; Müller et al., 2011;
15 Xiao et al., 2015). Here, we observe a remarkably lower correlation between PIPSO₂₅ values and spring sea ice
16 concentrations with a coefficient of determination $r^2 = 0.37$ for P_ZIPSO₂₅, $r^2 = 0.50$ for P_EIPSO₂₅ (Fig. 5a), $r^2 =$
17 0.31 for P_BIPSO₂₅, and $r^2 = 0.34$ for P_DIPSO₂₅ (Fig. 5b). The highest correlation is found between winter sea ice
18 concentrations and P_EIPSO₂₅ ($r^2 = 0.71$), and P_ZIPSO₂₅ ($r^2 = 0.62$, Fig. 5c). A weaker correlation is noted for the
19 sterol-based PIPSO₂₅ values (P_BIPSO₂₅: $r^2 = 0.52$; P_DIPSO₂₅: $r^2 = 0.42$, Fig. 5d).

20 The contour lines in Figure 4 a-d show the observed extent of 15 %, 30 %, 40 % and 50 % winter sea ice compared
21 to the PIPSO₂₅ values. In the northeastern part of the study area, the HBI triene based PIPSO₂₅ indices align well
22 with the contour lines of winter sea ice concentrations and depict the gradient from the marginally ice-covered
23 southern Drake Passage towards the intensively ice-covered Weddell Sea. In the southwestern part of the
24 Bransfield Strait, all PIPSO₂₅ indices suggest a higher sea ice cover than it is reflected in the satellite data. At
25 stations PS97/052 and PS97/053, off the continental slope, the absence of IPSO₂₅ is in conflict with the satellite
26 data depicting an average winter sea ice cover of 23 %. Earlier documentations that the IPSO₂₅ producing sea ice
27 diatom *Berkeleya adeliensis* favors land-fast ice communities in East Antarctica (Riaux-Gobin and Poulin, 2004)
28 and platelet ice occurring mainly in near coastal areas (Belt et al., 2016) could explain this mismatch between
29 biomarker and satellite data, which further strengthens the hypothesis that the application of IPSO₂₅ seems to be
30 confined to continental shelf or near-coastal and meltwater affected environments (Belt et al., 2016).



1 As photosynthesis is not possible and a release of sea ice diatoms from melting sea ice is highly reduced during
2 the Antarctic winter, the observation of a stronger correlation between recent winter sea ice concentrations and
3 PIPSO₂₅ sea ice estimates is unexpected. We hence suggest that this offset may be related to the fact that the
4 sediment samples integrate a longer time interval than is covered by satellite observations. Radiocarbon dating of
5 selected samples that contain calcareous material reveals considerable ages of 100 years BP in the vicinity of the
6 South Shetland Islands (station PS97/059-2) and 142 years BP at the Antarctic Sound (station PS1546-2, Table 3).
7 A significantly older age was determined for a sample of *N. Pachyderma* from station PS97/044-1 (4830 years
8 BP) in the Drake Passage. Bioturbation effects and uncertainties in reservoir ages potentially mask the ages of the
9 near-coastal samples.

10 Nevertheless, since also other published ages of surface sediments within the Bransfield Strait (Barbara et al.,
11 2013; Barnard et al., 2014; Etourneau et al., 2013; Heroy et al., 2008) are in the range of 0-270 years, we consider
12 that our surface samples likely reflect the paleoenvironmental conditions that prevailed during the last two
13 centuries (and not just the last 35 years covered by satellite observations). In the context of the rapid warming
14 during the last century (Vaughan et al., 2003) and the decrease of sea ice at the WAP (King, 2014; King and
15 Harangozo, 1998), we suggest that the biomarker data of the surface sediments relate to a spring sea ice cover,
16 which must have been enhanced compared to the recent (past 35 years) spring sea ice recorded via remote sensing.
17 Presumably, the average spring sea ice conditions over the past 200 years might have been similar to the modern
18 (past 35 years) winter conditions, which would explain the stronger correlation between PIPSO₂₅ sea ice estimates
19 and winter sea ice concentrations.

20

21 **4.4 Comparison of sea ice associated diatom species and biomarker data**

22 The diatoms preserved in sediments from the study area (Table 4) can be associated with open ocean and sea ice
23 conditions. North of the South Shetland Islands, the strong influence of the ACC is reflected in the high abundance
24 of open ocean diatom species such as *Fragilariopsis kerguelensis* and *Thalassiosira lentiginosa* (Esper et al.,
25 2010). The two diatom species *Fragilariopsis curta* and *Fragilariopsis cylindrus* – known to not produce HBI
26 (Belt et al., 2016; Damsté et al., 2004) – are used for the reconstruction of sea ice conditions (Gersonde and
27 Zielinski, 2000; Xiao et al., 2016). They mark the vicinity to sea ice (Buffen et al., 2007; Pike et al., 2008) and
28 indicate fast and melting ice, a stable sea ice margin and stratification due to melting processes and the occurrence
29 of seasonal sea ice. The high abundance of these species in our samples is in good agreement with high and
30 moderate IPSO₂₅ concentrations and PIPSO₂₅ values in the Bransfield Strait and around the South Shetland Islands,
31 respectively. The only HBI source diatom identified is the HBI Z-triene producing *Rhizosolenia hebetata* (Belt et



1 al., 2017), which is present in four samples in rather small amounts and does not show a relation to the measured
2 Z-triene values (Table 1 and 4). The source diatom of IPSO₂₅ *Berkeleya adeliensis* was not observed (or preserved)
3 in the samples, and we assume that other, hitherto unknown, producers may exist.

4 We applied the transfer function of Esper and Gersonde (2014a) to our samples to compare the different estimates
5 of sea ice cover based on biomarkers and diatoms. A strong positive correlation is found between the winter sea
6 ice (WSI) concentrations derived from diatoms and the PIPSO₂₅ indices based on HBI trienes (P_ZIPSO₂₅ with $r^2 =$
7 0.76; P_EIPSO₂₅ with $r^2 = 0.77$, Fig. 6a). The correlations of sterol-based PIPSO₂₅ values with WSI are slightly
8 lower but in the same range (P_BIPSO₂₅ with $r^2 = 0.74$; P_DIPSO₂₅ with $r^2 = 0.69$, Fig. 6b). A slightly weaker
9 correlation is noted for diatom- and satellite-based winter sea ice concentrations ($r^2 = 0.63$; Fig. 6c). Overall, the
10 diatom approach indicates higher sea ice concentrations than the satellite data and we observe an offset of up to
11 65 %. This may be due to different sources of satellite reference data used for the transfer function or also due to
12 the fact that the sediment samples integrate a longer time period with a higher sea ice cover than the satellite data
13 (see discussion in section 4.3).

14

15 **4.5 Application of PIPSO₂₅ as a semi-quantitative sea ice index**

16 Precise and, in particular, quantitative reconstructions of past sea ice coverage are crucial for a robust assessment
17 of feedback mechanisms in the ice-ocean-atmosphere system. While diatom transfer functions provide a valuable
18 tool, additional information on sea ice conditions in coastal ice-shelf proximal areas, which are often affected by
19 opal dissolution, are essential. The PIPSO₂₅ approach seems to be a promising step into this direction, though our
20 data obtained for the WAP are not yet sufficient for a full calibration. PIPSO₂₅, diatom and satellite sea ice data,
21 however, reveal strong positive correlations (Fig. 5 and 6) and depict similar gradients in sea ice cover. The
22 observed offset between satellite data and biomarker- and diatom-based sea ice estimates likely relates to the fact
23 that the instrumental records cover a significantly shorter or more recent time interval than the studied sediments.
24 The recent rapid warming along the WAP (Vaughan et al., 2003) hence complicates attempts to calibrate these
25 proxy data against observational data. The high correlation between diatom-derived winter sea ice concentrations
26 and PIPSO₂₅ values (Fig. 6a and b) may even argue for a calibration of the IPSO₂₅ index against diatom data and
27 a use of HBI trienes as phytoplankton marker. The robustness and reliability of such an approach, however, has to
28 be proven by means of a larger data set. Regarding the interpretation of PIPSO₂₅ in terms of sea ice coverage in
29 the study area, lower PIPSO₂₅ values (<0.15 for P_ZIPSO₂₅; <0.31 for P_EIPSO₂₅; <0.22 for P_BIPSO₂₅ and P_DIPSO₂₅)
30 roughly seem to reflect unconsolidated, drifting winter sea ice and a nearly ice-free spring season. Higher values



- 1 (>0.71 for $P_Z\text{IPSO}_{25}$; >0.9 $P_E\text{IPSO}_{25}$; >0.6 for $P_B\text{IPSO}_{25}$ and $P_D\text{IPSO}_{25}$) would refer to an extended winter sea ice
- 2 cover (up to 91 % in some years) lasting until summer.



1 **5 Conclusion**

2 The distribution of the sea ice biomarker IPSO₂₅ and related HBI trienes and sterols as well as diatoms in a suite
3 of surface sediments from the southern Drake Passage and the WAP reflects recent sea ice conditions reasonably
4 well. The herein established sea ice index PIPSO₂₅ indicates seasonal sea ice cover along the coast of the WAP
5 and in the Bransfield Strait, whereas mainly ice-free conditions prevail in the Drake Passage. In general, this
6 pattern is consistent with satellite-derived sea ice data and diatom-based sea ice estimates and we note that the
7 PIPSO₂₅ index seems a promising approach towards semi-quantitative sea ice reconstructions in the Southern
8 Ocean. The recent rapid warming in the study area, however, affects the comparability of proxy and satellite data.
9 The fact that the surface sediments integrate a significantly longer time interval than the remote sensing data
10 thwarts attempts to calibrate PIPSO₂₅ values against observed sea ice concentrations. Additional data from other
11 circum-Antarctic coastal (and distal) environments and investigations into potential calibration methods are
12 needed to further develop this index as a quantitative sea ice proxy.

13



1 **Data Availability**

2 All data can be found in this paper and will be available at the open access repository www.pangaea.de.

3

4 **Author contributions**

5 The study was conceived by MV and JM. Data collections and experimental investigations were done by MV
6 together with OE (diatoms), GM (radiocarbon dating), CH (satellite data), and ES (isotope data). MV wrote the
7 manuscript and did the visualizations. KF provided technical support. JM supervised the study. All authors
8 contributed to the interpretation and discussion of the results and the conclusion of this study.

9

10 **Competing interests**

11 None of the authors has a conflict of interest.

12

13 **Acknowledgement**

14 We thank the captain and crew of RV Polarstern cruise PS97, and the following supporters: Mandy Kiel
15 (technician), Lester Lembke-Jene (biology, dating), Liz Bonk and Hendrik Grotheer (from MICADAS), Max
16 Mues (sample preparation), Nicoletta Ruggieri (lab support), Walter Luttmer (lab support). Financial support was
17 provided through the Helmholtz Research grant VH-NG-1101.

18



1 **References**

- 2 Anderson, R. F., Ali, S., Bradtmiller, L. I., Nielsen, S. H. H., Fleisher, M. Q., Anderson, B. E. and Burckle, L. H.:
- 3 Wind-Driven Upwelling in the Southern Ocean and the Deglacial Rise in Atmospheric CO₂, *Science* (80-),
- 4 323(5920), 1443–1448, doi:10.1126/science.1167441, 2009.
- 5 Arrigo, K. R., Worthen, D. L., Lizotte, M. P., Dixon, P. and Dieckmann, G.: Primary Production in Antarctic Sea
- 6 Ice, *Science* (80-), 276, 394–397, doi:10.1126/science.276.5311.394, 1997.
- 7 Barbara, L., Crosta, X., Schmidt, S. and Massé, G.: Diatoms and biomarkers evidence for major changes in sea
- 8 ice conditions prior the instrumental period in Antarctic Peninsula, *Quat. Sci. Rev.*, 79, 99–110,
- 9 doi:10.1016/j.quascirev.2013.07.021, 2013.
- 10 Barbara, L., Crosta, X., Leventer, A., Schmidt, S., Etourneau, J., Domack, E. and Massé, G.: Environmental
- 11 responses of the Northeast Antarctic Peninsula to the Holocene climate variability, *Paleoceanography*, 31(1),
- 12 131–147, doi:10.1002/2015PA002785, 2016.
- 13 Bárcena, M. A., Gersonde, R., Ledesma, S., Fabrés, J., Calafat, A. M., Canals, M., Sierro, F. J. and Flores, J. A.:
- 14 Record of Holocene glacial oscillations in Bransfield Basin as revealed by siliceous microfossil assemblages,
- 15 *Antarct. Sci.*, 10(03), 269–285, doi:10.1017/S0954102098000364, 1998.
- 16 Barnard, A., Wellner, J. S. and Anderson, J. B.: Late Holocene climate change recorded in proxy records from a
- 17 Bransfield Basin sediment core, *Antarctic Peninsula, Polar Res.*, 33(1), doi:10.3402/polar.v33.17236, 2014.
- 18 Belt, S. T.: Source-specific biomarkers as proxies for Arctic and Antarctic sea ice, *Org. Geochem.*, 125, 277–298,
- 19 doi:10.1016/j.orggeochem.2018.10.002, 2018.
- 20 Belt, S. T. and Müller, J.: The Arctic sea ice biomarker IP 25 : a review of current understanding ,
- 21 recommendations for future research and applications in palaeo sea ice reconstructions, *Quat. Sci. Rev.*, 79, 9–
- 22 25, doi:10.1016/j.quascirev.2012.12.001, 2013.
- 23 Belt, S. T., Allard, W. G., Massé, G., Robert, J. M. and Rowland, S. J.: Highly branched isoprenoids (HBIs):
- 24 Identification of the most common and abundant sedimentary isomers, *Geochim. Cosmochim. Acta*, 64(22),
- 25 3839–3851, doi:10.1016/S0016-7037(00)00464-6, 2000.
- 26 Belt, S. T., Masse, G., Rowland, S. J., Poulin, M., Michel, C. and Leblanc, B.: A novel chemical fossil of palaeo sea
- 27 ice : IP 25, *Org. Geochem.*, 38, 16–27, doi:10.1016/j.orggeochem.2006.09.013, 2007.
- 28 Belt, S. T., Brown, T. A., Ringrose, A. E., Cabedo-Sanz, P., Mundy, C. J., Gosselin, M. and Poulin, M.: Quantitative
- 29 measurement of the sea ice diatom biomarker IP25 and sterols in Arctic sea ice and underlying sediments:



- 1 Further considerations for palaeo sea ice reconstruction, *Org. Geochem.*, 62, 33–45,
2 doi:10.1016/J.ORGGEOCHEM.2013.07.002, 2013.
- 3 Belt, S. T., Brown, T. A., Ampel, L., Cabedo-Sanz, P., Fahl, K., Kocis, J. J., Massé, G., Navarro-Rodriguez, A., Ruan,
4 J. and Xu, Y.: An inter-laboratory investigation of the Arctic sea ice biomarker proxy
5 IP<sub>25</sub</sub> in marine sediments: key outcomes and recommendations,
6 *Clim. Past*, 10(1), 155–166, doi:10.5194/cp-10-155-2014, 2014.
- 7 Belt, S. T., Cabedo-Sanz, P., Smik, L., Navarro-Rodriguez, A., Berben, S. M. P., Knies, J. and Husum, K.:
8 Identification of paleo Arctic winter sea ice limits and the marginal ice zone: Optimised biomarker-based
9 reconstructions of late Quaternary Arctic sea ice, *Earth Planet. Sci. Lett.*, 431, 127–139,
10 doi:10.1016/j.epsl.2015.09.020, 2015.
- 11 Belt, S. T., Smik, L., Brown, T. A., Kim, J. H., Rowland, S. J., Allen, C. S., Gal, J. K., Shin, K. H., Lee, J. I. and Taylor,
12 K. W. R.: Source identification and distribution reveals the potential of the geochemical Antarctic sea ice proxy
13 IPSO25, *Nat. Commun.*, 7, 1–10, doi:10.1038/ncomms12655, 2016.
- 14 Belt, S. T., Brown, T. A., Smik, L., Tatarek, A., Wiktor, J., Stowasser, G., Assmy, P., Allen, C. S. and Husum, K.:
15 Identification of C25 highly branched isoprenoid (HBI) alkenes in diatoms of the genus *Rhizosolenia* in polar and
16 sub-polar marine phytoplankton, *Org. Geochem.*, 110, 65–72, doi:10.1016/j.orggeochem.2017.05.007, 2017.
- 17 Belt, S. T., Brown, T. A., Smik, L., Assmy, P. and Mundy, C. J.: Sterol identification in floating Arctic sea ice algal
18 aggregates and the Antarctic sea ice diatom *Berkeleya adeliensis*, *Org. Geochem.*, 118, 1–3,
19 doi:10.1016/j.orggeochem.2018.01.008, 2018.
- 20 Berben, S. M. P., Husum, K., Cabedo-Sanz, P. and Belt, S. T.: Holocene sub-centennial evolution of Atlantic
21 water inflow and sea ice distribution in the western Barents Sea, *Clim. Past*, 10(1), 181–198, doi:10.5194/cp-10-
22 181-2014, 2014.
- 23 Buffen, A., Leventer, A., Rubin, A. and Hutchins, T.: Diatom assemblages in surface sediments of the
24 northwestern Weddell Sea, Antarctic Peninsula, *Mar. Micropaleontol.*, 62(1), 7–30,
25 doi:10.1016/J.MARMICRO.2006.07.002, 2007.
- 26 Burckle, L. H. and Cooke, D. W.: Late Pleistocene *Eucampia antarctica* Abundance Stratigraphy in the Atlantic
27 Sector of the Southern Ocean, *Micropaleontology*, 29(1), 6, doi:10.2307/1485648, 1983.
- 28 Cabedo-Sanz, P., Belt, S. T., Knies, J. and Husum, K.: Identification of contrasting seasonal sea ice conditions
29 during the Younger Dryas, *Quat. Sci. Rev.*, 79, 74–86, doi:10.1016/j.quascirev.2012.10.028, 2013.



- 1 Cárdenas, P., Lange, C. B., Vernet, M., Esper, O., Srain, B., Vorrath, M.-E., Ehrhardt, S., Müller, J., Kuhn, G., Arz,
2 H. W., Lembke-Jene, L. and Lamy, F.: Biogeochemical proxies and diatoms in surface sediments across the
3 Drake Passage reflect oceanic domains and frontal systems in the region, *Prog. Oceanogr.*,
4 doi:10.1016/j.pocean.2018.10.004, 2018.
- 5 Cavaliere, D. J., Parkinson, C. L., Gloersen, P. and Zwally, H. J.: Sea Ice Concentrations from Nimbus-7 SMMR and
6 DMSP SSM/I-SSMIS Passive Microwave Data, Version 1, Boulder, Color. USA, doi:10.5067/8GQ8LZQVL0VL,
7 1996.
- 8 Collins, L. G., Allen, C. S., Pike, J., Hodgson, D. A., Weckström, K. and Massé, G.: Evaluating highly branched
9 isoprenoid (HBI) biomarkers as a novel Antarctic sea-ice proxy in deep ocean glacial age sediments, *Quat. Sci.*
10 *Rev.*, 79, 87–98, doi:10.1016/j.quascirev.2013.02.004, 2013.
- 11 Crosta, X., Pichon, J.-J. and Burckle, L. H.: Application of modern analog technique to marine Antarctic diatoms:
12 Reconstruction of maximum sea-ice extent at the Last Glacial Maximum, *Paleoceanography*, 13(3), 284–297,
13 doi:10.1029/98PA00339, 1998.
- 14 Damsté, J. S. S., Muyzer, G., Abbas, B., Rampen, S. W., Massé, G., Allard, W. G., Belt, S. T., Robert, J. M.,
15 Rowland, S. J., Moldowan, J. M., Barbanti, S. M., Fago, F. J., Denisevich, P., Dahl, J., Trindade, L. A. F. and
16 Schouten, S.: The Rise of the Rhizosolenid Diatoms, *Science* (80-.), 304(5670), 584–587,
17 doi:10.1126/science.1096806, 2004.
- 18 Denis, D., Crosta, X., Barbara, L., Massé, G., Renssen, H., Ther, O. and Giraudeau, J.: Sea ice and wind variability
19 during the Holocene in East Antarctica: insight on middle–high latitude coupling, *Quat. Sci. Rev.*, 29(27–28),
20 3709–3719, doi:10.1016/J.QUASCIREV.2010.08.007, 2010.
- 21 Esper, O. and Gersonde, R.: New tools for the reconstruction of Pleistocene Antarctic sea ice, *Palaeogeogr.*
22 *Palaeoclimatol. Palaeoecol.*, 399, 260–283, doi:10.1016/J.PALAEO.2014.01.019, 2014a.
- 23 Esper, O. and Gersonde, R.: Quaternary surface water temperature estimations: New diatom transfer functions
24 for the Southern Ocean, *Palaeogeogr. Palaeoclimatol. Palaeoecol.*, 414, 1–19,
25 doi:10.1016/J.PALAEO.2014.08.008, 2014b.
- 26 Esper, O., Gersonde, R. and Kadagies, N.: Diatom distribution in southeastern Pacific surface sediments and
27 their relationship to modern environmental variables, *Palaeogeogr. Palaeoclimatol. Palaeoecol.*, 287(1–4), 1–
28 27, doi:10.1016/J.PALAEO.2009.12.006, 2010.
- 29 Etourneau, J., Collins, L. G., Willmott, V., Kim, J. H., Barbara, L., Leventer, A., Schouten, S., Sinninghe Damsté, J.



- 1 S., Bianchini, A., Klein, V., Crosta, X. and Massé, G.: Holocene climate variations in the western Antarctic
2 Peninsula: Evidence for sea ice extent predominantly controlled by changes in insolation and ENSO variability,
3 *Clim. Past*, 9(4), 1431–1446, doi:10.5194/cp-9-1431-2013, 2013.
- 4 Fetterer, F., Knowles, K., Meier, W., Savoie, M. and Windnagel, A. K.: Sea Ice Index, Version 3, NSIDC Natl. Snow
5 Ice Data Cent., doi:10.7265/N5K072F8, 2017.
- 6 Fütterer, D. K.: Die Expedition ANTARKTIS-VI mit FS Polarstern 1987/1988 (The Expedition ANTARKTIS-VI of RV
7 Polarstern in 1987/88), Alfred-Wegener-Institut für Polar- und Meeresforschung, Bremerhaven, Germany.,
8 1988.
- 9 Gersonde, R. and Zielinski, U.: The reconstruction of late Quaternary Antarctic sea-ice distribution — the use of
10 diatoms as a proxy for sea-ice, *Palaeogeogr. Palaeoclimatol. Palaeoecol.*, 162, 263–286, doi:10.1016/S0031-
11 0182(00)00131-0, 2000.
- 12 Gonçalves-Araujo, R., de Souza, M. S., Tavano, V. M. and Garcia, C. A. E.: Influence of oceanographic features
13 on spatial and interannual variability of phytoplankton in the Bransfield Strait, Antarctica, *J. Mar. Syst.*, 142, 1–
14 15, doi:10.1016/J.JMARSYS.2014.09.007, 2015.
- 15 Hancke, K., Lund-Hansen, L. C., Lamare, M. L., Højlund Pedersen, S., King, M. D., Andersen, P. and Sorrell, B. K.:
16 Extreme Low Light Requirement for Algae Growth Underneath Sea Ice: A Case Study From Station Nord, NE
17 Greenland, *J. Geophys. Res. Ocean.*, 123(2), 985–1000, doi:10.1002/2017JC013263, 2018.
- 18 Heroy, D. C., Sjunneskog, C. and Anderson, J. B.: Holocene climate change in the Bransfield Basin, Antarctic
19 Peninsula: evidence from sediment and diatom analysis, *Antarct. Sci.*, 20(01), 69–87,
20 doi:10.1017/S0954102007000788, 2008.
- 21 Hobbs, W. R., Massom, R., Stammerjohn, S., Reid, P., Williams, G. and Meier, W.: A review of recent changes in
22 Southern Ocean sea ice, their drivers and forcings, *Glob. Planet. Change*, 143, 228–250,
23 doi:10.1016/j.gloplacha.2016.06.008, 2016.
- 24 Hofmann, E. E., Klinck, J. M., Lascara, C. M. and Smith, D. A.: Water mass distribution and circulation west of
25 the Antarctic Peninsula and including Bransfield Strait, in *Foundations for Ecological Research West of the*
26 *Antarctic Peninsula*, edited by R. . Ross, E. E. Hofmann, and L. B. Quetin, pp. 61–80, American Geophysical
27 Union (AGU), Washington, D. C., 1996.
- 28 Kanazawa, A., Yoshioka, M. and Teshima, S.-I.: The occurrence of brassicasterol in the diatoms, *Cyclotella nana*
29 and *Nitzschia closterium*, *Bull. Japanese Soc. Sci. Fish.*, 37, 889–903, 1971.



- 1 King, J.: A resolution of the Antarctic paradox, *Nature*, 505(7484), 491–492, doi:10.1038/505491a, 2014.
- 2 King, J. C. and Harangozo, S. A.: Climate change in the western Antarctic Peninsula since 1945: observations
3 and possible causes, *Ann. Glaciol.*, 27, 571–575, doi:10.3189/1998AoG27-1-571-575, 1998.
- 4 Lamy, F.: The expedition PS97 of the research vessel POLARSTERN to the Drake Passage in 2016, *Reports Polar
5 Mar. Res.*, 7'01, 1–571, doi:10.2312/BzPM_0702_2016, 2016.
- 6 Leventer, A.: The fate of Antarctic “sea ice diatoms” and their use as paleoenvironmental indicators, in
7 *Antarctic Research Series*, edited by M. P. Lizotte and K. R. Arrigo, pp. 121–137, American Geophysical Union
8 (AGU), 1998.
- 9 Liu, J., Curry, J. A. and Martinson, D. G.: Interpretation of recent Antarctic sea ice variability, *Geophys. Res.
10 Lett.*, 31(2), 2000–2003, doi:10.1029/2003GL018732, 2004.
- 11 Massé, G., Belt, S. T., Crosta, X., Schmidt, S., Snape, I., Thomas, D. N. and Rowland, S. J.: Highly branched
12 isoprenoids as proxies for variable sea ice conditions in the Southern Ocean, *Antarct. Sci.*, 23(05), 487–498,
13 doi:10.1017/S0954102011000381, 2011.
- 14 Minzoni, R. T., Anderson, J. B., Fernandez, R. and Wellner, J. S.: Marine record of Holocene climate, ocean, and
15 cryosphere interactions: Herbert Sound, James Ross Island, Antarctica, *Quat. Sci. Rev.*, 129, 239–259,
16 doi:10.1016/j.quascirev.2015.09.009, 2015.
- 17 Müller, J. and Stein, R.: High-resolution record of late glacial and deglacial sea ice changes in Fram Strait
18 corroborates ice–ocean interactions during abrupt climate shifts, *Earth Planet. Sci. Lett.*, 403, 446–455,
19 doi:10.1016/j.epsl.2014.07.016, 2014.
- 20 Müller, J., Massé, G., Stein, R. and Belt, S. T.: Variability of sea-ice conditions in the Fram Strait over the past
21 30,000 years, *Nat. Geosci.*, 2(11), 772–776, doi:10.1038/ngeo665, 2009.
- 22 Müller, J., Wagner, A., Fahl, K., Stein, R., Prange, M. and Lohmann, G.: Towards quantitative sea ice
23 reconstructions in the northern North Atlantic: A combined biomarker and numerical modelling approach,
24 *Earth Planet. Sci. Lett.*, 306(3–4), 137–148, doi:10.1016/J.EPSL.2011.04.011, 2011.
- 25 Müller, J., Werner, K., Stein, R., Fahl, K., Moros, M. and Jansen, E.: Holocene cooling culminates in sea ice
26 oscillations in Fram Strait, *Quat. Sci. Rev.*, 47, 1–14, doi:10.1016/j.quascirev.2012.04.024, 2012.
- 27 Nichols, P. D., Volkman, J. K., Palmisano, A. C., Smith, G. A. and White, D. C.: Occurrence of an Isoprenoid C25
28 diunsaturated alkene and high neutral lipid content in Antarctic Sea-Ice Diatom communities, *J. Phycol.*, 24, 90–
29 96, 1988.



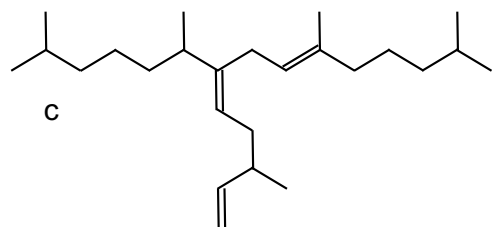
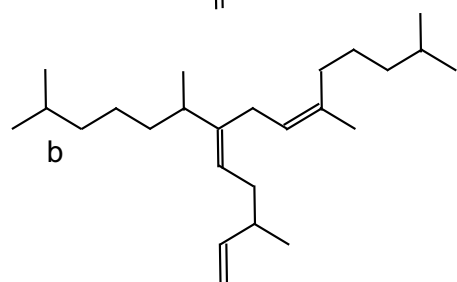
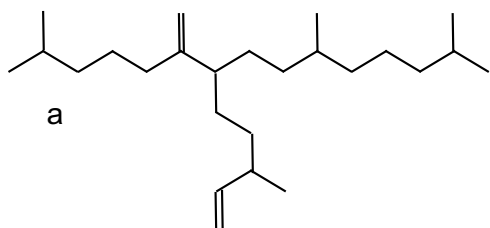
- 1 Orsi, A. H., Smethie, W. M. and Bullister, J. L.: On the total input of Antarctic waters to the deep ocean: A
2 preliminary estimate from chlorofluorocarbon measurements, *J. Geophys. Res.*, 107, 31-,
3 doi:10.1029/2001JC000976, 2002.
- 4 Parkinson, C. L.: Trends in the length of the Southern Ocean sea-ice season, 1979-99, *Ann. Glaciol.*, 34(1), 435–
5 440, doi:10.3189/172756402781817482, 2002.
- 6 Parkinson, C. L. and Cavalieri, D. J.: Antarctic sea ice variability and trends, 1979–2010, *Cryosph.*, 6, 871–880,
7 doi:10.5194/tc-6-871-2012, 2012.
- 8 Pike, J., Allen, C. S., Leventer, A., Stickley, C. E. and Pudsey, C. J.: Comparison of contemporary and fossil diatom
9 assemblages from the western Antarctic Peninsula shelf, *Mar. Micropaleontol.*, 67(3–4), 274–287,
10 doi:10.1016/J.MARMICRO.2008.02.001, 2008.
- 11 Riaux-Gobin, C. and Poulin, M.: Possible symbiosis of *Berkeleya adeliensis* Medlin, *Synedropsis fragilis*
12 (Manguin) Hasle et al. and *Nitzschia lecontei* Van Heurck (bacillariophyta) associated with land-fast ice in
13 Adélie Land, Antarctica, *Diatom Res.*, 19(2), 265–274, doi:10.1080/0269249X.2004.9705874, 2004.
- 14 Rontani, J.-F., Belt, S. T., Vaultier, F., Brown, T. A. and Massé, G.: Autoxidative and Photooxidative Reactivity of
15 Highly Branched Isoprenoid (HBI) Alkenes, *Lipids*, 49(5), 481–494, doi:10.1007/s11745-014-3891-x, 2014a.
- 16 Rontani, J.-F., Belt, S. T., Brown, T. A., Vaultier, F. and Mundy, C. J.: Sequential photo- and autoxidation of
17 diatom lipids in Arctic sea ice, *Org. Geochem.*, 77, 59–71, doi:10.1016/j.orggeochem.2014.09.009, 2014b.
- 18 Rontani, J. F., Belt, S. T., Vaultier, F. and Brown, T. A.: Visible light induced photo-oxidation of highly branched
19 isoprenoid (HBI) alkenes: Significant dependence on the number and nature of double bonds, *Org. Geochem.*,
20 42(7), 812–822, doi:10.1016/j.orggeochem.2011.04.013, 2011.
- 21 Sangrà, P., Gordo, C., Hernández-Arencibia, M., Marrero-Díaz, A., Rodríguez-Santana, A., Stegner, A., Martínez-
22 Marrero, A., Pelegrí, J. L. and Pichon, T.: The Bransfield current system, *Deep Sea Res. Part I Oceanogr. Res.*
23 *Pap.*, 58(4), 390–402, doi:10.1016/J.DSR.2011.01.011, 2011.
- 24 Schrader, H. and Gersonde, R.: Diatoms and silicoflagellates, in *Micropaleontological Methods and Techniques -*
25 *An Exercise on an Eight Meter Section of the Lower Pliocene of Capo Rossello, Sicily, Utrecht*
26 *Micropaleontological Bulletins*, vol. 17, edited by W. J. Zachariasse, W. R. Riedel, A. Sanfilippo, R. R. Schmidt, M.
27 J. Brolsma, H. J. Schrader, R. Gersonde, M. M. Drooger, and J. A. Broekman, pp. 129–176., 1978.
- 28 Scott, F. J. and Thomas, D. P.: Diatoms, in *Antarctic Marine Protists*, p. 563, Australian Biological Resources
29 Study, Canberra & Hobart., 2005.



- 1 Sinninghe Damsté, J. S., Rijpstra, W. I. C., Coolen, M. J. L., Schouten, S. and Volkman, J. K.: Rapid sulfurisation of
2 highly branched isoprenoid (HBI) alkenes in sulfidic Holocene sediments from Ellis Fjord, Antarctica, *Org.*
3 *Geochem.*, 38(1), 128–139, doi:10.1016/j.orggeochem.2006.08.003, 2007.
- 4 Smik, L., Belt, S. T., Lieser, J. L., Armand, L. K. and Leventer, A.: Distributions of highly branched isoprenoid
5 alkenes and other algal lipids in surface waters from East Antarctica: Further insights for biomarker-based
6 paleo sea-ice reconstruction, *Org. Geochem.*, 95, 71–80, doi:10.1016/J.ORGGEOCHEM.2016.02.011, 2016a.
- 7 Smik, L., Cabedo-Sanz, P. and Belt, S. T.: Semi-quantitative estimates of paleo Arctic sea ice concentration
8 based on source-specific highly branched isoprenoid alkenes: A further development of the PIP 25 index, *Org.*
9 *Geochem.*, 92, 63–69, doi:10.1016/j.orggeochem.2015.12.007, 2016b.
- 10 Stein, R., Fahl, K. and Müller, J.: Proxy Reconstruction of Cenozoic Arctic Ocean Sea-Ice History: from IRD to
11 IP25, *Polarforschung*, 82(1), 37–71, 2012.
- 12 Stein, R., Fahl, K., Gierz, P., Niessen, F. and Lohmann, G.: Arctic Ocean sea ice cover during the penultimate
13 glacial and the last interglacial, *Nat. Commun.*, 8(1), 373, doi:10.1038/s41467-017-00552-1, 2017.
- 14 Stuiver, M., Reimer, P. J. and Reimer, R. W.: *Calib 7.1*, 2018.
- 15 Vaughan, D. G., Marshall, G. J., Connolley, W. M., Parkinson, C., Mulvaney, R., Hodgson, D. A., King, J. C.,
16 Pudsey, C. J. and Turner, J.: Recent Rapid Regional Climate Warming on the Antarctic Peninsula, *Clim. Change*,
17 60(3), 243–274, doi:10.1023/A:1026021217991, 2003.
- 18 Volkman, J. K.: Sterols in microorganisms, *Appl. Microbiol. Biotechnol.*, 60(5), 495–506, doi:10.1007/s00253-
19 002-1172-8, 2003.
- 20 Wacker, L., Bonani, G., Friedrich, M., Hajdas, I., Kromer, B., Némec, M., Ruff, M., Suter, M., Synal, H.-A. and
21 Vockenhuber, C.: MICADAS: Routine and High-Precision Radiocarbon Dating, *Radiocarbon*, 52(02), 252–262,
22 doi:10.1017/S0033822200045288, 2010.
- 23 Xiao, W., Esper, O. and Gersonde, R.: Last Glacial - Holocene climate variability in the Atlantic sector of the
24 Southern Ocean, *Quat. Sci. Rev.*, 135, 115–137, doi:10.1016/j.quascirev.2016.01.023, 2016.
- 25 Xiao, X., Fahl, K., Müller, J. and Stein, R.: Sea-ice distribution in the modern Arctic Ocean: Biomarker records
26 from trans-Arctic Ocean surface sediments, *Geochim. Cosmochim. Acta*, 155, 16–29,
27 doi:10.1016/J.GCA.2015.01.029, 2015.
- 28



1 **Figures**

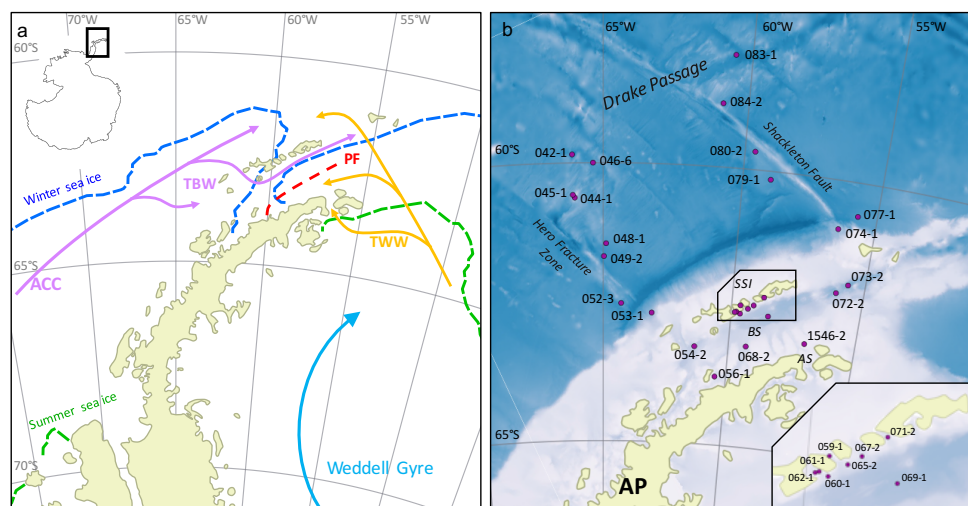


2

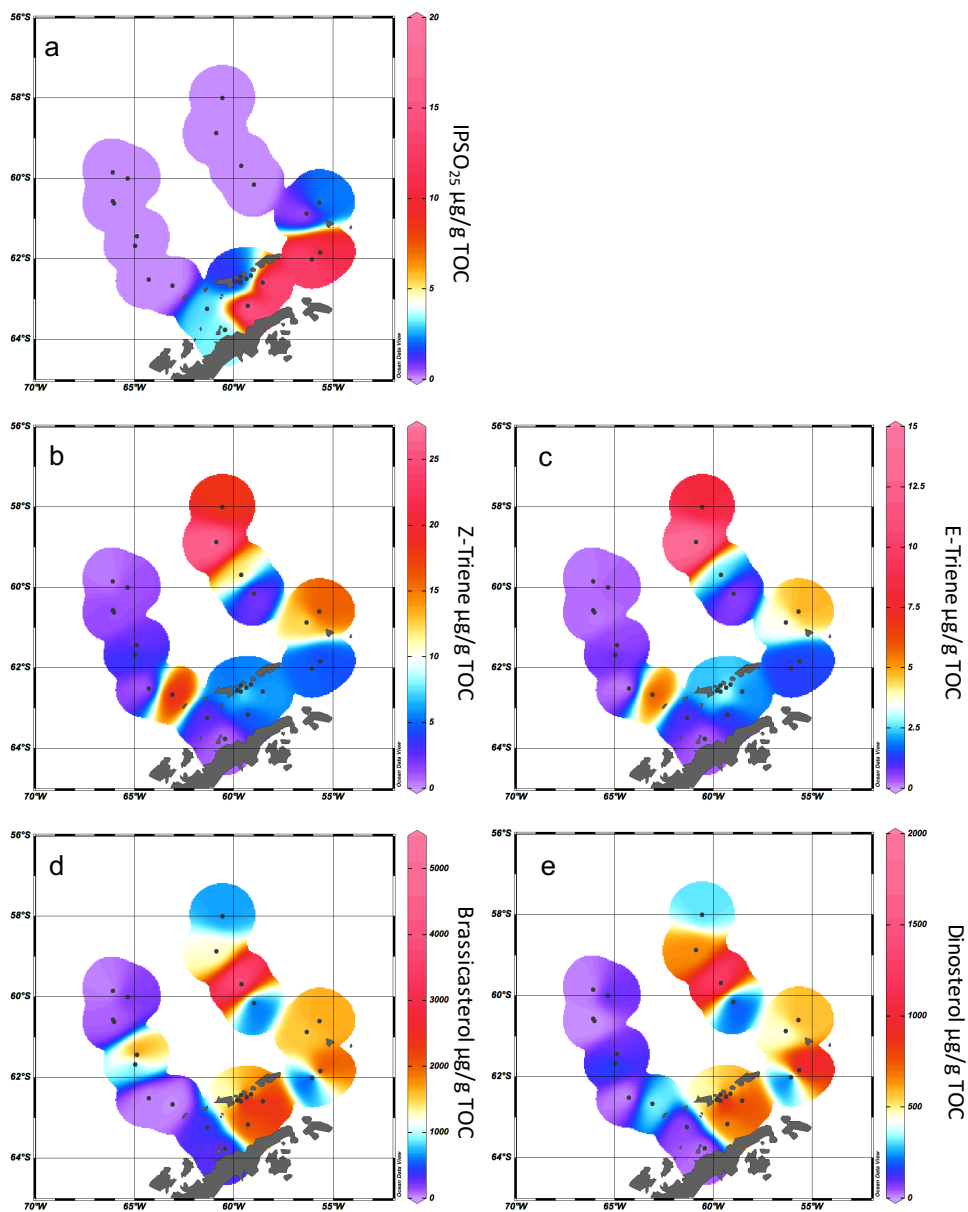
3

Figure 1: The molecular structures of a) IPSO₂₅, b) the HBI Z-triene, and c) the HBI E-triene.

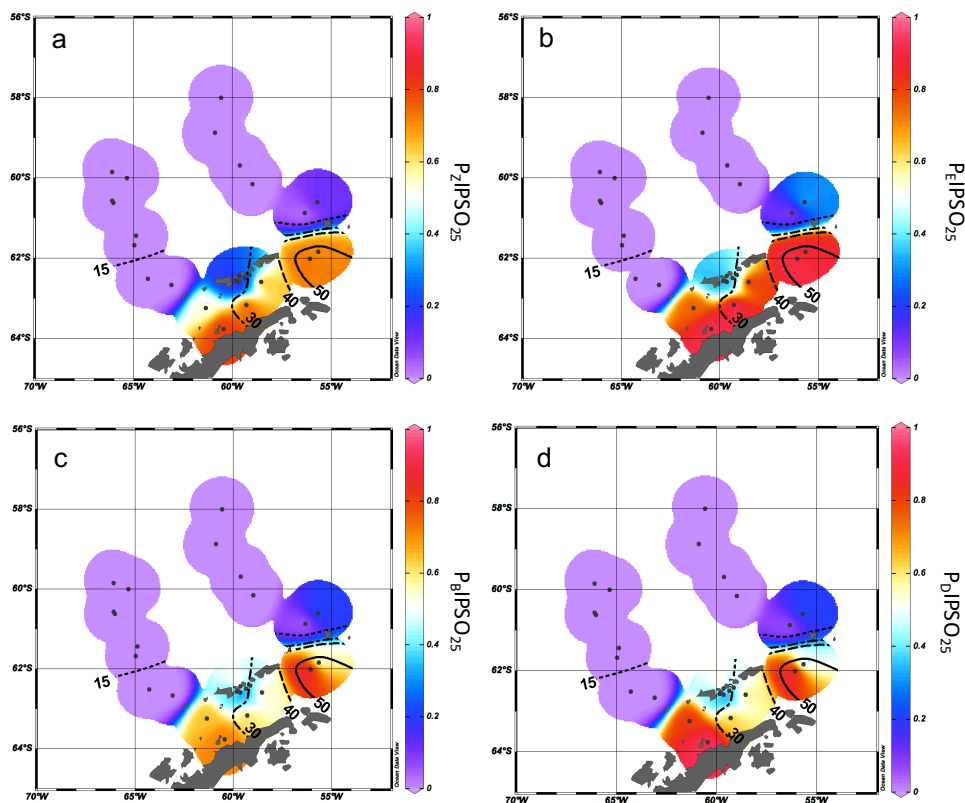
4



1
2 **Figure 2:** a) Oceanographic setting of the study area (modified after Hofmann et al., 1996; Sangrà et al., 2011) with
3 ACC = Antarctic Circumpolar Current, TBW = Transitional Bellingshausen Water, TWW = Transitional Weddell
4 Water, and PF = Peninsula Front. The mean extent of winter and summer sea ice (1981 and 2010) is taken from the
5 National Snow and Ice Data Center (Fetterer et al., 2017). b) The bathymetric map of the study area with locations of
6 all stations; AP = Antarctic Peninsula, AS = Antarctic Sound, BS = Bransfield Strait, and SSI = South Shetland Islands.
7 A detailed station map at the South Shetland Islands is integrated.
8 The overview maps were done with QGIS 3.0 from 2018 and the bathymetry was taken from GEBCO_14 from 2015.
9



1
2 **Figure 3: Distribution of a) IPSO₂₅, b) HBI Z-triene, c) HBI E-triene, d) brassicasterol, and e) dinosterol concentrations**
3 **normalized to TOC. All distribution plots were made with Ocean Data View 4.7.10 (2017).**
4

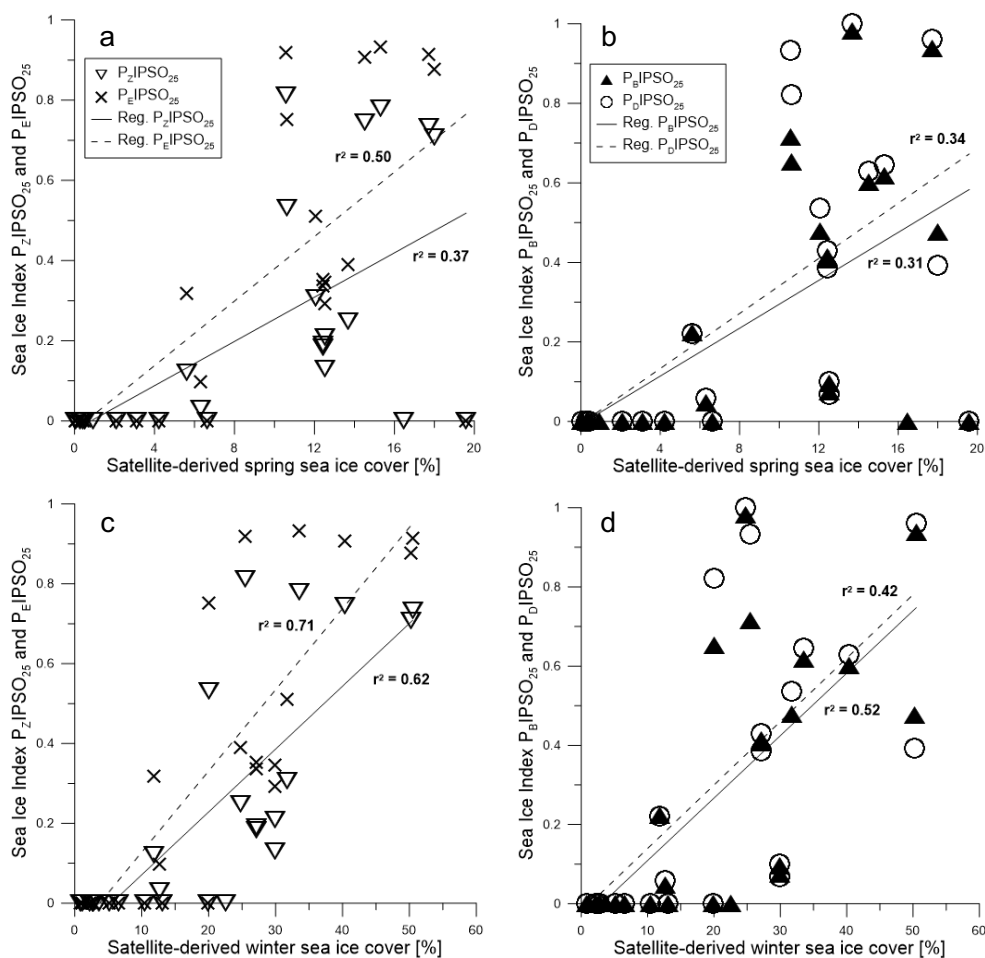


1

2 **Figure 4: Distribution of a) P_ZIPSO_{25} , b) $P_{EIPSO_{25}}$, c) $P_{BIPSO_{25}}$, and d) $P_{DIPSO_{25}}$ values in the study area. The extent**
3 **of 15 %, 30 %, 40 % and 50 % satellite sea ice concentrations during winter is added as contour lines.**

4

5



1

2

Figure 5: Scatter plots of satellite spring sea ice concentrations and a) P_Z IPSO₂₅ (triangles, solid regression line) and

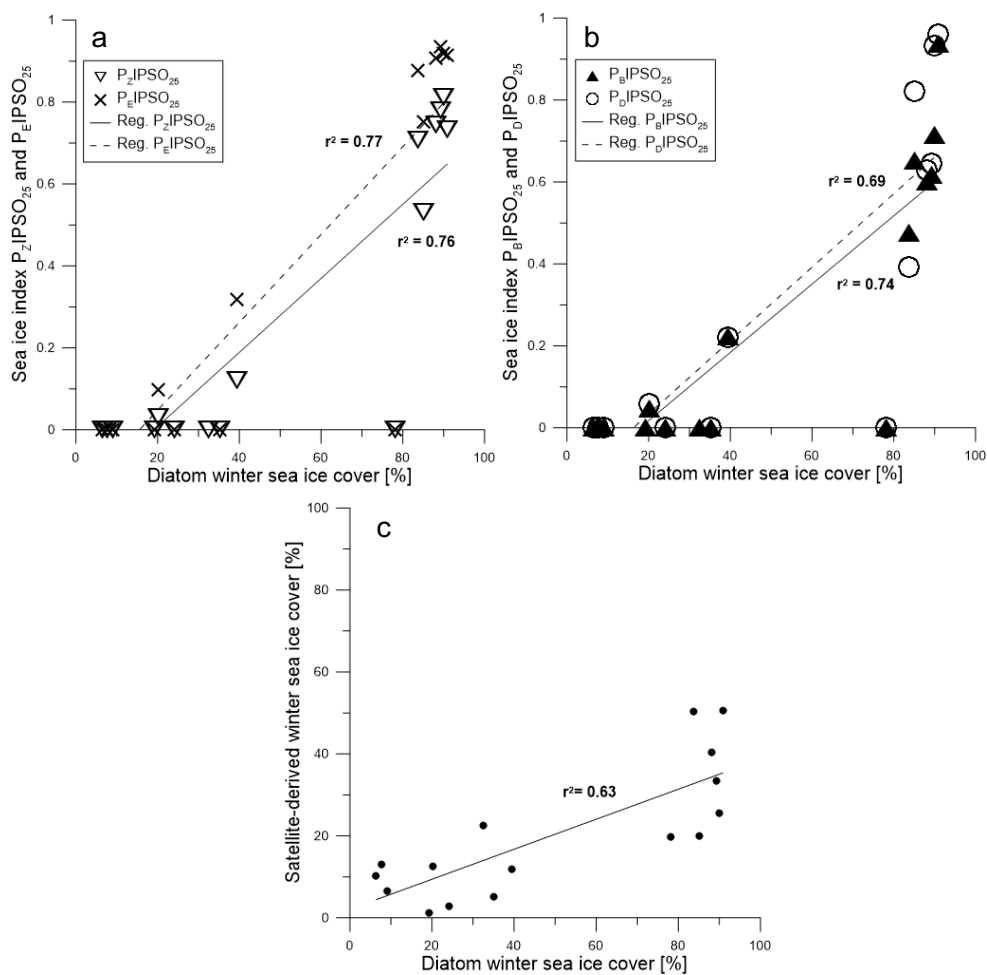
3

P_E IPSO₂₅ (crosses, dashed regression line) and b) P_B IPSO₂₅ (black triangles, solid regression line) and P_D IPSO₂₅ (circles,

4

dashed regression line). All scatter plots were done with Grapher™ 13.

5



1
2 **Figure 6:** Scatter plots of a) P_ZIPSO_{25} (triangles, solid regression line) and P_EIPSO_{25} (crosses, dashed regression line)
3 and b) P_BIPSO_{25} (black triangles, solid regression line) and P_DIPSO_{25} (circles, dashed regression line) against diatom
4 derived winter sea ice concentrations. c) Scatter plot of diatom transfer function based winter sea ice concentrations
5 and satellite winter sea ice concentrations.



- 6 Tables
- 7 Table 1: Coordinates of sample stations with water depth, concentrations of IPSO₂₅, Z- and E-trienes, brassicasterol and dinosterol normalized to TOC, $\delta^{13}\text{C}$ values for IPSO₂₅, and values
- 8 of sea ice indices PIPSO₂₅ based on the Z- and E-triene, brassicasterol and dinosterol. Concentrations below the detection limit are expressed as 0. The PIPSO₂₅ could not be calculated
- 9 where IPSO₂₅ and the phytoplankton marker is absent (blank fields).



Station	Lon [°E]	Lat [°N]	Water Depth [m]	IPSO ₂₅ /TOC [µg/g TOC]	HBI-Z/Triene/TOC [µg/g TOC]	HBI-E/Triene/TOC [µg/g TOC]	Brassi-casterol/TOC [µg/g TOC]	Dino-sterol/TOC [µg/g TOC]	δ ¹³ C of IPSO ₂₅ [‰]	P ₁ IPSO ₂₅	P ₂ IPSO ₂₅	P ₃ IPSO ₂₅	P ₄ IPSO ₂₅	P ₅ IPSO ₂₅
PS97/042-1	-66.10	-59.85	4172	0	0.333	0.152	12.997	0	0.000	0.000	0.000	0.000	0.000	0.000
PS97/044-1	-66.03	-60.62	1203	0	1.080	0	143.688	0	0.000	0.000	0.000	0.000	0.000	0.000
PS97/045-1	-66.10	-60.57	2292	0	1.531	0.386	36.902	0	0.000	0.000	0.000	0.000	0.000	0.000
PS97/046-6	-65.36	-60.00	2803	0	1.359	0.291	214.634	101.809	0.000	0.000	0.000	0.000	0.000	0.000
PS97/048-1	-64.89	-61.44	3455	0	2.085	0.375	1859.609	73.532	0.000	0.000	0.000	0.000	0.000	0.000
PS97/049-2	-64.97	-61.67	3752	0	3.924	0.851	719.155	178.446	0.000	0.000	0.000	0.000	0.000	0.000
PS97/052-3	-64.30	-62.51	2890	0	0.679	0	26.554	0	0.000	0.000	0.000	0.000	0.000	0.000
PS97/053-1	-63.10	-62.67	2021	0	19.350	5.948	13.356	332.868	0.000	0.000	0.000	0.000	0.000	0.000
PS97/054-2	-61.35	-63.24	1283	3.033	2.675	1.000	337.686	48.579	-14.741	0.531	0.752	0.652	0.820	0.820
PS97/056-1	-60.45	-63.76	633	3.232	0.752	0.290	268.190	17.158	-10.3 ± 0.9	0.811	0.918	0.716	0.932	0.932
PS97/059-1	-59.66	-62.44	354	0.835	2.523	1.305	3.386	0.0002	0.000	0.249	0.390	0.981	0.999	0.999
PS97/060-1	-59.65	-62.59	462	1.934	12.937	4.693	5017.437	1983.750	0.000	0.130	0.292	0.074	0.066	0.066
PS97/061-1	-59.80	-62.56	467	1.018	4.341	1.870	302.356	119.512	0.000	0.190	0.352	0.413	0.383	0.383
PS97/062-1	-59.86	-62.57	477	0.907	4.044	1.787	276.372	88.272	0.000	0.183	0.337	0.407	0.428	0.428
PS97/065-2	-59.36	-62.49	480	2.416	9.184	4.549	4788.292	1587.309	0.000	0.208	0.347	0.095	0.100	0.100
PS97/067-2	-59.15	-62.42	793	1.785	4.038	1.710	406.567	113.728	0.000	0.307	0.511	0.478	0.533	0.533
PS97/068-2	-59.30	-63.17	794	16.206	4.558	1.152	2096.690	653.977	-14.1 ± 0.6	0.780	0.934	0.617	0.643	0.643
PS97/069-1	-58.55	-62.59	1642	17.814	6.115	1.824	2472.025	774.345	-12.6 ± 0.4	0.744	0.907	0.601	0.626	0.626
PS97/072-2	-56.07	-62.01	1992	13.689	4.997	1.277	192.625	40.686	-13.6 ± 0.3	0.733	0.915	0.937	0.961	0.961
PS97/073-2	-55.66	-61.84	2624	10.369	4.283	1.451	2388.458	1180.752	0.000	0.708	0.877	0.476	0.390	0.390
PS97/074-1	-56.35	-60.87	1831	0.371	12.075	3.409	1539.629	438.073	0.000	0.030	0.098	0.048	0.058	0.058
PS97/077-1	-55.71	-60.60	3587	2.267	16.356	4.874	1647.616	589.731	0.000	0.122	0.317	0.223	0.219	0.219
PS97/079-1	-59.00	-60.15	3539	0	1.893	0.510	479.917	154.400	0.000	0.000	0.000	0.000	0.000	0.000
PS97/080-2	-59.64	-59.68	3113	0	12.021	2.705	4019.003	1329.129	0.000	0.000	0.000	0.000	0.000	0.000
PS97/083-1	-60.57	-58.00	3756	0	18.256	8.280	686.502	308.610	0.000	0.000	0.000	0.000	0.000	0.000
PS97/084-2	-60.88	-58.87	3617	0	26.857	13.871	1245.652	648.474	0.000	0.000	0.000	0.000	0.000	0.000



11 **Table 2: Seasonal sea ice concentrations from satellite observations for spring, summer, autumn and winter with**
 12 **standard deviations.**

Station	Sea Ice Spring [%]	Sea Ice Spring StDev [%]	Sea Ice Summer [%]	Sea Ice Summer StDev [%]	Sea Ice Autumn [%]	Sea Ice Autumn StDev [%]	Sea Ice Winter [%]	Sea Ice Winter StDev [%]
PS97/042-1	0.04	0.19	0.00	0.00	0.01	0.05	1.14	5.00
PS97/044-1	0.92	3.25	0.02	0.23	0.00	0.00	3.67	9.38
PS97/045-1	0.52	2.08	0.01	0.08	0.00	0.04	2.65	7.81
PS97/046-6	0.29	1.35	0.00	0.00	0.00	0.00	2.84	8.55
PS97/048-1	4.22	8.52	0.00	0.00	0.00	0.00	10.36	18.17
PS97/049-2	6.65	11.85	0.00	0.00	0.00	0.04	13.02	19.91
PS97/052-3	16.48	21.62	0.40	2.95	0.04	0.31	22.59	24.94
PS97/053-1	19.59	23.59	0.29	2.45	0.04	0.35	19.86	24.13
PS97/054-2	10.62	15.18	0.44	0.79	0.76	2.62	20.06	20.72
PS97/056-1	10.55	16.21	4.73	3.25	2.77	4.44	25.47	23.02
PS97/059-1	13.67	16.13	4.23	2.25	5.03	5.48	24.77	20.33
PS97/060-1	12.53	16.84	1.87	2.15	5.43	9.24	29.93	22.05
PS97/061-1	12.43	16.18	1.86	2.07	4.15	7.30	27.14	21.31
PS97/062-1	12.43	16.18	1.86	2.07	4.15	7.30	27.14	21.31
PS97/065-2	12.53	16.84	1.87	2.15	5.43	9.24	29.93	22.05
PS97/067-2	12.08	17.22	0.82	1.88	5.60	10.10	31.74	22.69
PS97/068-2	15.30	19.35	4.89	3.40	6.44	10.45	33.49	23.13
PS97/069-1	14.51	19.85	0.40	2.34	7.83	13.78	40.41	24.27
PS97/072-2	17.74	22.74	1.46	5.38	16.69	20.35	50.49	25.09
PS97/073-2	17.99	23.28	1.81	6.14	16.43	19.85	50.29	26.01
PS97/074-1	6.30	13.65	0.02	0.12	0.55	2.29	12.65	19.30
PS97/077-1	5.60	12.20	0.04	0.13	0.77	2.99	11.83	17.81
PS97/079-1	3.10	8.91	0.03	0.27	0.01	0.12	6.50	15.49
PS97/080-2	2.08	7.52	0.01	0.08	0.00	0.04	5.14	14.17
PS97/083-1	0.03	0.23	0.00	0.00	0.00	0.04	0.87	4.27
PS97/084-2	0.40	2.21	0.00	0.00	0.00	0.04	2.23	9.59

13

14 **Table 3: Details of the radiocarbon dates and calibrated ages.**

Sample Name	AWI-No.	Material	F ¹⁴ C ± error	Conventional ¹⁴ C age [a]	Calibrated age (cal BP) [a]
PS97/044-1	1657.1.1	N. pachyderma	0.5076	5447 ± 111	4830
PS97/059-2	1434.1.1	calcareous	0.8507	1299 ± 49	100
PS1546-2	1602.1.1	Moll.-Echinod	0.8456	1347 ± 64	142

15

16

